Dual polarization DFB fiber lasers as optical phase-locked microwave sources in the 1-10 GHz range

M. Guionie, Ludovic Frein, François Bondu, Anthony Carré, Goulc'Hen Loas, Emmanuel Pinsard, Benoît Cadier, Mehdi Alouini, Marco Romanelli, Marc Vallet, et al.

Dual-polarization DFB fiber lasers as optical phase-locked microwave sources in the 1-10 GHz range

M. Guionie[1], L. Frein[1], F. Bondu[1], A. Carré[1], G. Loas[1], E. Pinsard[2], B. Cadier[2], M. Alouini[1], M. Romanelli[1], M.Vallet[1], M. Brunel[1]
[1]Univ Rennes, CNRS, Institut FOTON - UMR 6082, F-35000 Rennes, France;
[2]iXblue Photonics, rue Paul Sabatier, 22300 Lannion, France

ABSTRACT

Fully fibered microwave-optical sources at 1.5 µm are studied experimentally. It is shown that the beat note between two orthogonally polarized modes of a distributed-feedback fiber laser can be efficiently stabilized using an optical phase-locked loop that uses the pump-power induced-birefringence as actuator. Beat notes at 1 GHz and 10 GHz of Erbium doped fiber laser are successfully stabilized to a reference synthesizer, passing from the 3 kHz free-running linewidth to a stabilized sub-Hz linewidth, with a phase noise as low as –75 dBc/Hz at 100 Hz offset from the carrier. An Erbium-Ytterbium co-doped fiber laser is also investigated and successfully stabilized. Such dual-frequency stabilized lasers could provide compact integrated components for RF and microwave photonics applications.

Keywords: Fiber lasers, microwave sources, dual-frequency,DFB

1. INTRODUCTION

Since their first demonstration in 1964, performances of fiber lasers have been improved in many ways (e.g. reduced linewidth, high output power). Besides their beam quality due to the confinement of laser radiation in the structure, their major advantages are compactness, ruggedness, and ease of integration. Fiber lasers are hence appealing sources for a wide variety of applications[1]. Distributed feedback (DFB) fiber lasers are usually known to be single frequency but it has long been observed that DFB lasers can sustain the oscillation of two orthogonal polarizations at different frequencies[2–4]. Such dual-frequency DFB fiber lasers were used as sensors[5,6], and may be promising as heterodyne sources in the field of microwave photonics[7–10].However, in the context of optical distribution of local oscillators for instance, we can wonder whether DFB fiber laser can be used to realize a stable continuous-wave microwave source. Stabilization of the beat frequency against a reference is then mandatory. Elasto-optical effects, induced by torsion[8] or compression[9], have already been used to control the beat frequency of dual-polarization fiber lasers, but phase-locked stabilization to a reference oscillator has never been performed. More precisely, we are interested in an optical phase-locked loop (OPLL) where the DFB fiber laser acts as a voltage-controlled oscillator (VCO) driven by the laser pump power.

Pump-induced thermal effects may become useful for noise reduction or locking in the case of diode-pumped short-cavity solid-state lasers. For example, phase-locking microchip lasers was demonstrated with a feedback on the pump-power of one laser with respect to the other[11]. Besides, simultaneous intensity and frequency noise reduction was obtained in a non-planar ring oscillator[12]. Also, locking a single-frequency erbium microchip laser to a molecular line was realized by a simple modulation-demodulation technique through the pump power[13]. In all these examples, small temperature variations lead to important frequency shifts due to the thermo-optical effect in the short cavity. The low dimensions also leads to reasonable kHz lock-in bandwidths[11,13]. While in Ref. 14 the role of pump-induced thermal effects on the frequency switching in ytterbium-doped DBR fiber lasers was demonstrated theoretically and experimentally, the pump-induced beat tuning effect has not been exploited previously in fiber lasers. Here we focus on erbium-doped DFB fiber lasers emitting in the 1.5 µm wavelength region. We find experimentally that minute differential refractive index changes provided by the pump power offer a satisfactory VCO effect, in both amplitude and bandwidth, which in turn permit to build a robust servo-locking loop.

We first detail in Section 2 the experimental set-up for OPLL and laser characteristics, with emphasis on the beat note study, of a laser operating with a 1 GHz frequency difference. Section 3 is then devoted to the OPLL based on

pump-power control. In Section 4 and 5 we extend the same principle to a laser emitting a 10 GHz beat note and on Er^{3+}:Yb^{3+}-codoped lasers respectively. Finally, conclusions are given in Section 6.

2. DUAL-POLARIZATION DFB FIBER LASERS

The experimental set-up for OPLL is shown in Figure 1. We have investigated different samples of erbium-doped and erbium-ytterbium co-doped silica fiber lasers, all being made with a distributed-feedback (DFB) structure. The Bragg gratings are photo-induced using the phase-mask technique with a pulsed, un-polarized, UV laser. The dual-polarization lasers studied here bear different grating profiles that are detailed below. In particular we will show results obtained with samples emitting beat notes at around 1 GHz (labeled 1G), at 10 GHz (labeled 10G) and at 300 MHz (labeled 0.3G). The lasers are spliced to single-mode fibers (cut-off 900 nm) on both sides. The lasers are pumped at 980 nm on the output coupler side through a 980/1550 wavelength-division multiplexer. The laser output is transmitted through an isolator, a polarization controller (PC), and a polarizer, to the analysis instruments. The system is entirely single-mode (non PM) fibered. In the following, we concentrate our analysis on the dual-frequency performance of the DFB lasers, in order to define a suitable phase-locked loopfor beat note stabilization, either at 1 GHz, 10 GHz or 300 MHz.

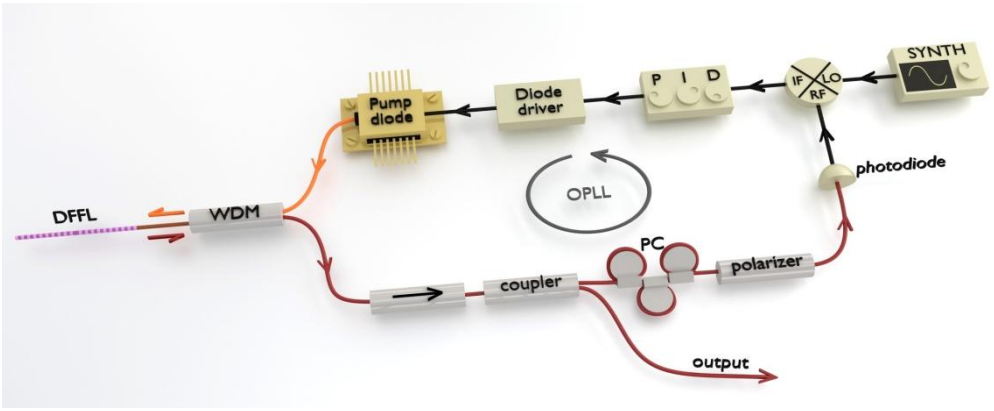

Figure 1. Optical phase-locked loop (OPLL) experimental set-up. DFFL: dual-frequency fiber laser; WDM, pump-signal coupler; PC, polarization controller; LO, local oscillator.

Let us detail the characteristics of sample 1G. The active medium is made with a 35 mm-long erbium-doped fiber, whose cladding diameter is 80 µm, and whose absorption is 11.3 dB/m at 1530 nm (the concentration is low enough to prevent any self-pulsing operation). The FBG is photo-induced at 193 nm, its central wavelength is λ_B= 1547.3 nm, its length is L_B= 30.5 mm, and its strength is κ= 390 m^{-1}. The resulting calculated effective length is L_{eff}= 2.6 mm. A π phase-shift is made at 18 mm from the beginning of the grating, leading to mirror intensity transmissions of –57 dB and –34 dB. Due to the photo-induced birefringence of the fiber, the phase-shifted grating sustains two polarization-resolved resonances at the center of the stop band. This is verified experimentally by characterizing the spectral transmission of the component without pumping, using a high-resolution optical spectrum analyzer (OSA) containing a built-in tunable laser source. As can be seen in Figure 2(a), the polarization-mode wavelength difference is 8 pm (1 GHz), while the width of the stop band is 200 pm (25 GHz). Note that the weakness of the two resonances is here due to absorption of the tunable probe by the un-pumped erbium ions. The wavelength difference $\Delta\lambda$ can be directly linked to the birefringence Δn by $\Delta\lambda/\lambda_B=\Delta n/n$. We can thus deduce $\Delta n= 7.5\ 10^{-6}$. This value is typical of DFB fiber lasers based on standard, i.e. non-PM, fiber, in agreement with the typical residual anisotropy induced by the photo-inscription process[15]. Depending on the sample under test, birefringence values between $6.8\ 10^{-6}$ (0.9 GHz) and $1.1\ 10^{-5}$ (1.5 GHz) have been found.

The fiber laser is pumped by a laser diode emitting 145 mW at 980 nm. The pump power at laser threshold is 2 mW and the laser emits at 1547 nm a total output power of 100 µW at 120 mW pumping power. The emitted optical spectrum corresponds to the dual-resonance bands of the FBG, and the frequency difference is measured to be 1.02 GHz at room temperature (Figure 2(b)). We verify that the two orthogonally polarized optical modes have the same pump threshold and are emitted with quite balanced powers (Figure 2(c)). The PC setting is chosen such that behind the polarizer, the high-bandwidth photodiode detects the dual-polarization beat note. Figure 3(a-b) presents the electrical spectrum of the beat over different spans and resolution bandwidths of the electrical spectrum analyzer (ESA). We verify that pure dual-frequency operation gives the radio-frequency tone at 1 GHz (Figure 3(a)). A zoom in this peak shows the free-running

3 kHz line-width of the beat note (Figure 3(b)). We observe a very stable beat power, with a typical 3% amplitude fluctuation (rms) over a few hours.

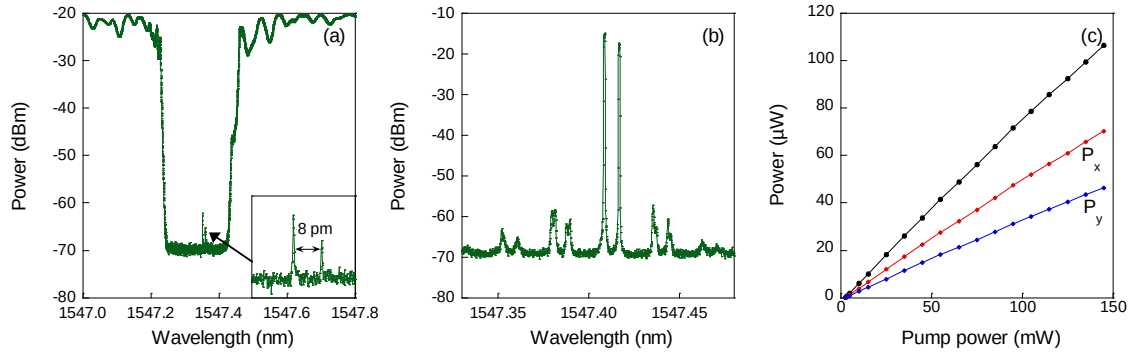

Figure 2.Optical spectra of sample 1G.(a) Un-pumped DFB transmission spectrum. Insert: zoom on the dual-mode structure. (b) Laser spectrum showing the two frequencies with a 1 GHz (8 pm) difference; pump power 59 mW (130 mA). (c) Total power (black) and resolved in polarization (red and blue curves). The threshold power is about 2 mW.

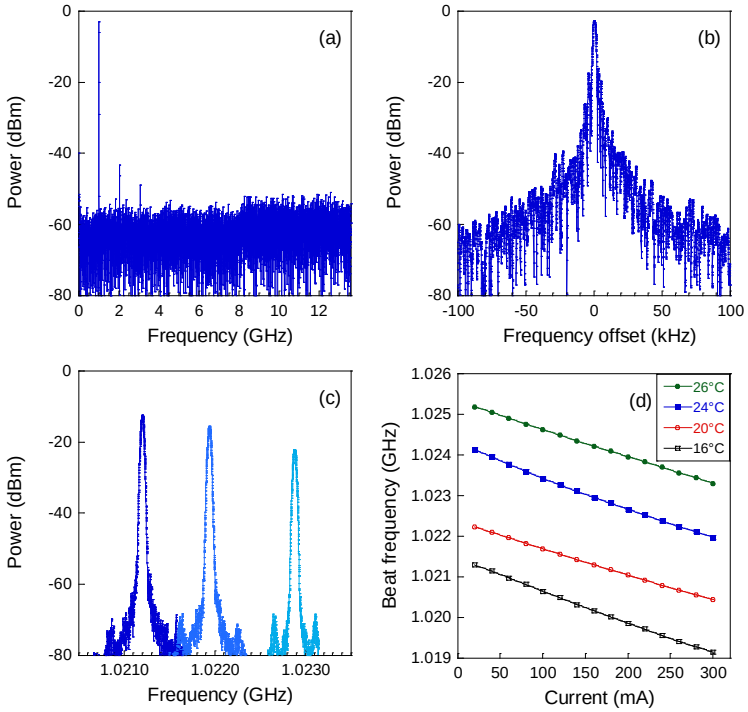

Figure 3. DFFL beat note at 1 GHz. (a) Span 13.6 GHz, RBW 3 MHz, spurious harmonics due to detection electronics, pump power 114 mW (250 mA). (b) Span 200 kHz, RBW 2 kHz, sweep time 100 ms. (c) Pump-power induced tuning: from right to left 45 mW (100 mA), 94 mW (200 mA), 144 mW(300 mA). (d)Beat note vs pump current at different laser temperatures.

3. OPTICAL PHASE-LOCKED LOOP

3.1 OPLL design at 1GHz

We first investigate the temperature tuning. The DFB fiber laser temperature is controlled by means of a thermo-electric Peltier device. Using the high-resolution OSA, we measure a thermal response of about 4 pm/K for each optical frequency in the 14-30°C temperature range. The beat frequency also depends on temperature. We monitor the beat thermal drift using the ESA, and find that the thermal response depends on the operating point (temperature and pump power). The important point is that, at a fixed pump power, the beat frequency stays within ±4 MHz in a ±5 K

temperature range around room temperature. In laboratory environment, without any temperature control, the drift is thus limited to about 2 MHz over a few hours. Second, we measure tuning characteristics provided by the pump power level. In contrast with the outside temperature control, it appears that the pump power gives a robust and reproducible means to control the beat frequency. Indeed, we find a DC response of the beat frequency to pump current change of –7 kHz/mA, as shown in Figure 3(c)-(d), quite independently of the laser temperature (linear fits yield slopes between –6.7 and –7.3 kHz/mA). Considering our pump diode, the power-to-frequency tuning curve then has a typical slope of –20 kHz/mW. It follows that pump power variations could be sufficient to counteract the environmental drifts. In the context of a phase-locked loop (PLL), the laser is a "voltage"-controlled oscillator (VCO) at the beat frequency, where "voltage" accounts for the pump power. The VCO gain is mainly related to the thermal heating induced by pump absorption. As a result, the VCO effect is expected to be limited in bandwidth. Nevertheless, as will be seen in the following, it allows us to build an efficient PLL.

The OPLL is implemented as follows. The 11 GHz-bandwidth photodiode is followed by a DC block, a 3 dB attenuator, and by a 30 dB-gain amplifier. This RF signal is mixed with the local oscillator (LO) provided by a synthesizer at 1 GHz whose output power is 10 dBm. At the mixer output, the error signal feeds a loop filter with proportional gain and integrator stages whose parameters are freely adjustable. The resulting signal is added to the DC current driving the pump diode (see Figure 1). In our set-up the diode driver has a gain of 0.65 A/V. Our loop filter consists in a proportional gain of 23 dB. It is worthwhile to mention that the laser itself acts as an integrator stage since it converts the correction signal into a frequency shift.

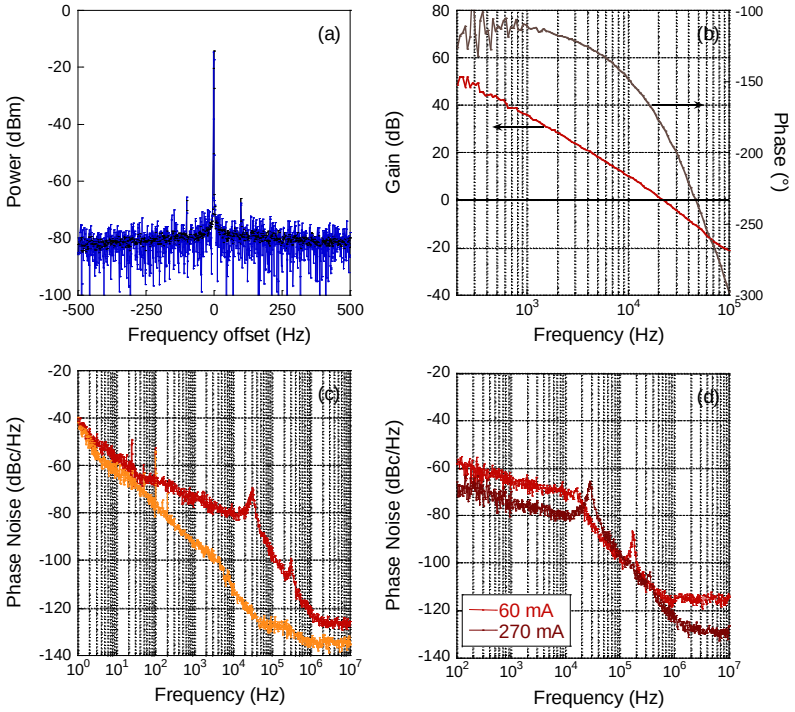

Figure 4. Locked beat note at 1 GHz. (a) Electrical spectrum (blue, single sweep; black average 10); Span 1 kHz, RBW 1 Hz, VBW 10 Hz, sweep 4.2 s. (b) Open-loop transfer function (red, gain; grey, phase). (c) Phase noise spectra (red, locked beat note; orange, LO). Pump power 92 mW (200 mA). (d) Phase noise spectra of 1G at two different pump current (red, 60 mA (25 mW); brown, 270 mA (123 mW)).

3.2 Results

When the loop is closed, the beat note can be locked. Figure 4(a) shows the stabilized spectrum. The measured line-width is 1 Hz (Full-Width at Half-Maximum), limited by the resolution bandwidth of our ESA. We measure a 1.5 MHz tracking range. Under our laboratory conditions, the beat then stays locked for days.

The open-loop transfer function can then be observed from closed-loop measurement using a low-signal network analyzer. This instrument is inserted between the mixer output and the loop filter input. The resulting Bode diagram is shown in Figure 4(b), giving insight to the low-frequency behavior of the pump-controlled oscillator. The smooth gain

decrease is due to the thermal response of the FBG laser, where the non-radiative relaxation of erbium ions in the fiber core is dominant. Indeed, we verified independently that the other loop elements have a flat gain up to at least 200 kHz. Thus the loop bandwidth (unit gain frequency) can be adjusted with the loop proportional gain. Under our experimental conditions, we can push the loop bandwidth (unit-gain frequency) up to 22 kHz. The corresponding phase noise is displayed in Figure 4(c). We measure a typical –65 dBc/Hz at 100 Hz offset and almost –80 dBc/Hz at 10 kHz offset from carrier. The small bump at around 300 kHz comes from the laser relaxation oscillations (intensity noise). For comparison the orange curve in Figure 4(c) plots the direct LO measurement. The beat and LO phase noises are almost equal at low frequencies, showing the stabilization and noise reduction effect of the OPLL. Besides, we observe a slight resonance at the unit-gain frequency (22 kHz) showing that the loop is close to the stability limit in this case. Finally, the loop gain also depends on the pump current, because the beat note amplitude is proportional to the laser output power. This is evidenced in Figure 4(d), where phase noise spectra at 60 mA and 270 mA of pump current are shown. The noise floor is reduced at higher power, but the loop resonance peak then gets stronger.

3.3 Calculation method for the free-running phase noise

In order to compare the closed-loop phase noise with the free-running beat note phase noise, we proceed as follows. We note that the free-running phase noise is not directly measurable by our phase noise measurement bench, because the fluctuations of the carrier frequency are too large at low frequency. However, we can deduce it from (i) the open-loop transfer function and (ii) the stabilized phase noise spectrum. .

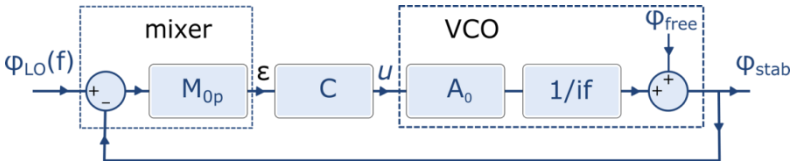

Figure 5. Model of the OPLL.

Block diagram of Figure 5 shows the complete loop. The error signal ε at the output of the mixer is proportional to the difference between the synthesizer phaseφ_{LO} and the closed-loop phase of the VCOφ_{stab}. M_0 is the peak value of the mixer gain (in V/rad). C is the transfer function of the loop filter (PID). u is the correction signal at the VCO input. A_0 is the VCO gain in MHz/V. The transfer function of the loop is then given by: $G_o = M_0 C A_0 \frac{1}{if}$. Go has been measured (Figure 4(b)), and the power spectral densities $S\varphi_{LO}$ and $S\varphi_{stab}$ of the local oscillator and stabilized VCO, respectively, can be retrieved from the phase noise spectra (Figure 4(c)). One can then deduce the power spectral density of the free-running VCO (labeled $S\varphi_{free}$) from the following equation:

$$Sf_{stab} = \left|\frac{1}{1+G_{bo}}\right|^2 Sf_{free} + \left|\frac{G_{bo}}{1+G_{bo}}\right|^2 Sf_{LO}, \quad (1)$$

where $S\varphi_{LO}$, $S\varphi_{stab}$, and $S\varphi_{free}$ are in rad/Hz². Since it can be assumed that $S\varphi_{free} > |G_{bo}|^2 S\varphi_{LO}$ we finally find:

$$Sf_{free} = \left|1+G_{bo}\right|^2 Sf_{stab}. \quad (2)$$

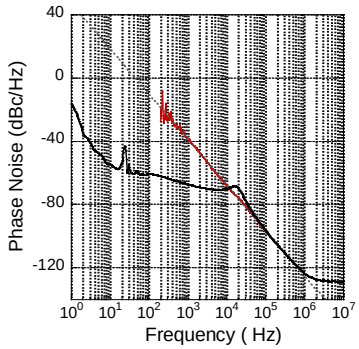

Figure 6. Phase noise spectra (black, locked beat note; red, free beat note; dotted, logarithmic adjustment with a slope of –28.7 dB/dec).

We used Equation (2) to calculate the phase noise of free-running beat note. Figure 6 compares free-running and stabilized phase noises of our laser under the same conditions. It is interesting to note that the fit to the free-running beat noise yields a slope close to –30 dB per decade, in agreement with previous studies[8].

4. LOCKING AT 10 GHZ

In this section we briefly discuss the extension to our pump-based OPLL to a dual-frequency fiber laser presenting a higher-frequency beat note. We consider another DFB sample, labeled 10G, that is based on the same glass as sample 1G, but has notable processing differences. The active medium is made with a 50 mm-long erbium-doped fiber, whose cladding diameter is 125 µm, and whose absorption is 11.1 dB/m at 1530 nm. The FBG is photo-induced at 248 nm, its central wavelength is λ_B = 1533 nm, its length is L_B = 41 mm, and its strength is κ = 275 m^{-1}. The resulting calculated effective length is L_{eff} = 3.3 mm. A π phase-shift is made at 27 mm from the beginning of the grating, leading to mirror intensity transmissions of –59 dB and –28 dB. While the birefringence is of the same order of magnitude as sample 1G, we have observed dual-frequency operation with one frequency at the center of the stop band, as usual, and another at the edge of the stop band, 10.2 GHz apart (see the optical transfer function in Figure7(a), and the emitted optical spectrum in Figure 7(b)). Figure 7(a) shows the polarization-resolved transfer function, with dotted lines showing the resonances that are observed to oscillate when the DFB is pumped. The beat note is reproduced in Figure 8, within a 26 GHz window in Figure 8(a), and a close-up in Figure 8(b) showing a kHz-scale free-running linewidth similar to the 1G sample. While the reason for this 10 GHz-beat oscillation is still unclear, we use this sample as a test device for a microwave OPLL based on the pump-power effect.

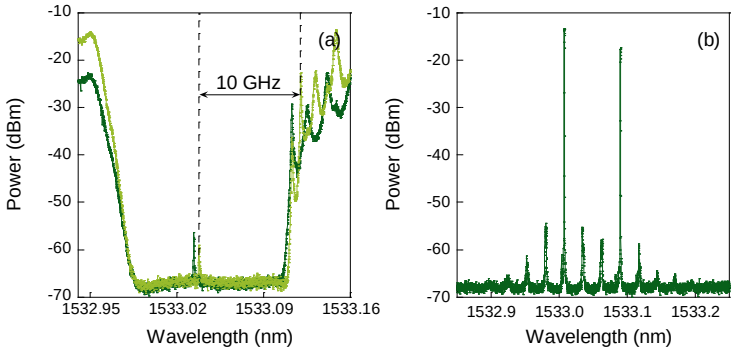

Figure 7. Optical spectrum of sample 10 G. (a) Transmission spectrum of cross polarization (un-pumped). (b) Emitted laser spectrum.

Laser 10G presents roughly the same pump threshold and output power as laser 1G. An important difference is that the VCO gain is measured to be 0.5 MHz/mA in this case, which is much higher than for sample 1G. We then used a low noise, low gain (1 mA/V) diode driver. We also had to upgrade both mixer and LO for operation at 10 GHz. Loop filter adjustments then lead to a proportional gain of 35 dB.

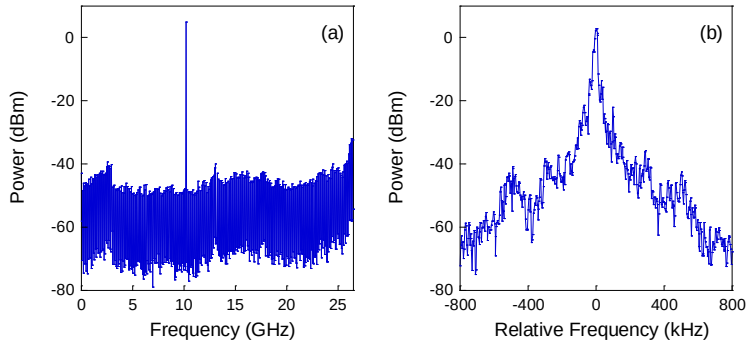

Figure 8. Beat note spectrum at 10 GHz. (a) Span 26 GHz, RBW 3 MHz. (b) Span 1.6 MHz, RBW 20 kHz.

As in case 1G, the laser beat at 10 GHz can be efficiently captured and locked, as shown in Figure 9(a). The open-loop transfer function can be observed from in-loop measurement. The resulting Bode diagram is shown in Figure 9(b),

where one can measure an open-loop 50 dB gain at low frequency and a unit-gain frequency of 37 kHz. In these conditions, the phase noise spectrum is displayed in Figure 9(c). The close-to-carrier phase noise is limited by the LO, while the intermediate frequency band shows lower phase noise than before, due to the low-noise diode driver. A phase noise plateau is measured at –75 dBc/Hz below 20 kHz offset from carrier. Finally the tracking range is 4 MHz, which again permits to maintain the beat locked for days in the laboratory environment. As for 1G, we calculate the phase noise of free beat note laser (Figure 9(c)). We observe at 1 kHz a 40 dB reduction of the phase noise with the PLL.

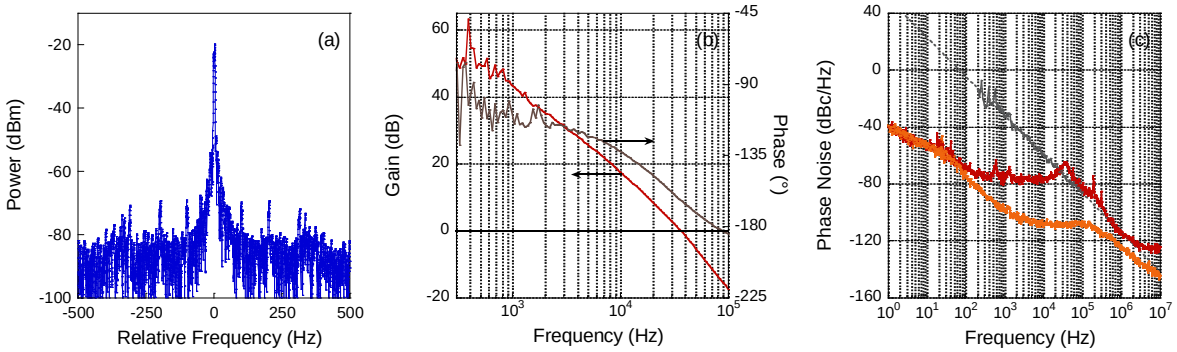

Figure 9. 10 GHz beat stabilization. (a) Electrical spectrum; Span 1 kHz ; RBW 1 Hz ; VBW 1 Hz.(b) Open-loop transfer function (red, gain; grey, phase). (c) Phase noise spectra (red, stabilized beat note; orange, measurement noise floor; grey, free-running beat note; dotted, logarithmic adjustment with a slope of -27.4 dB/dec).

5. Er:YbDUAL-FREQUENCY FIBER LASERS

In this section, we present some results obtained with a DFB fiber laser based on Er^{3+}:Yb^{3+}-codoping. The active medium is made with a 30 mm-long doped fiber, whose cladding diameter is 125 µm. The FBG is photo-induced at 193 nm, its central wavelength is λ_B = 1548 nm, its length is L_B = 28 mm, and its strength is κ = 362 m^{-1}. The resulting calculated effective length is L_{eff} = 2.8 mm. A π phase-shift is made at 16 mm from the beginning of the grating, leading to mirror intensity transmissions of –43 dB and –32 dB. Yb^{3+} doping prevents from Er-Erion clustering, leading to a higher Er doping concentrations without self-pulsing effects, and hence to higher output power[16–18]. The output power of these laser samples is in the 7 mW range (to be compared to 100 µW for the erbium-doped lasers described above). Figure 10(a) shows that the output power is saturated beyond 7mW.

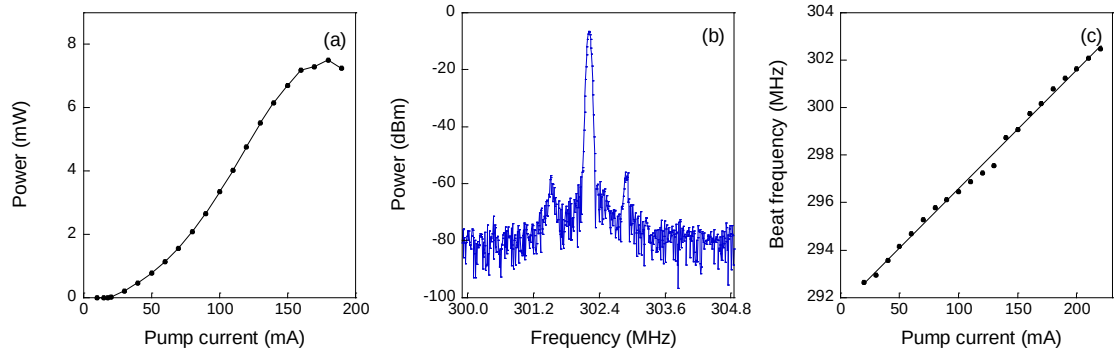

Figure 10. DFFL beat note at 0.3 GHz. (a) Total laser power curves. (b) Beat note spectrum at 300 MHz; Span 5 MHz ; RBW 50 kHz ; VBW 50 kHz; side-bands at around ±600 kHz offset are due to relaxation oscillation intensity noise. (c) Pump-power induced tuning.

We find experimentally that the laser emission spectrum consists in orthogonally polarized lines separated by 2.4 pm (0.3 GHz). Lower birefringence than sample 1G may be due to different sample compositions. For example, Figure 10(b)-(c) shows the beat note spectrum at 300 MHz and its tuning curve via the pump power. We measured a slope of 50 kHz/mA. Besides, laser 0.3G presents the same pump threshold as laser 1G and 10G. Because of the VCO gain, as 10G, we used a low noise, low gain (1 mA/V) diode driver. We also used the same mixer as 1G and the same LO as 10G stabilization. The best loop stability is obtained when the filter mixed proportional gain, an integrator and a differentiator.

In the same way as 1G and 10G, the laser 0.3G can be efficiently captured and locked, as shown in Figure 11(a). The Bode diagram of the open-loop transfer function is shown in Figure 11(b), where one can read an open-loop 56 dB gain at low frequency and a unit-gain frequency of 28 kHz. In these conditions, we measure the phase noise which is displayed in Figure 11(c). We observe a phase noise plateau around –80 dBc/Hz with a minimum at –95 dBc/Hz. For frequencies smaller than 100 Hz, the phase noise is limited by the LO. As for 1G and 10G, we calculate the phase noise of free-running beat note laser (Figure 11(c)). We observe at 10 kHz a 18 dB reduction of phase noise with PLL.

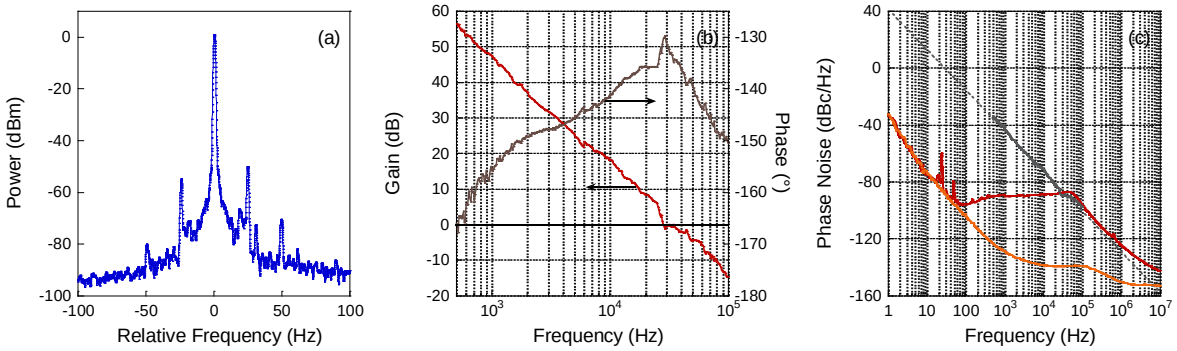

Figure 11. 300 MHz beat stabilization. (a) Electrical spectrum; Span 200 Hz ; RBW 1 Hz ; VBW 1 Hz. (b) Open-loop transfer function (red, gain; grey, phase). (c) Phase noise spectra (red, stabilized beat note; orange, measurement noise floor; grey, free beat note; dotted, logarithmic adjustment with a slope of –28.4 dB/dec).

6. CONCLUSION

Our experiments area demonstration of beat note phase-noise reduction in dual-frequency DFB erbium-doped and erbium-ytterbium co-doped fiber lasers. We have implemented a simple optical phase-locked loop on dual-frequency DFB lasers that uses the pump power as the laser actuator. Beat notes at 1 GHz and 10 GHz were successfully stabilized on the long-term, with a phase noise as low as –75 dBc/Hz at 100 Hz offset frequency. Beat note at 300 MHz were also successfully stabilized with a phase noise as low as –95 dBc/Hz at 100 Hz, with different PID loop parameters. The method may apply to other compact dual-polarization fiber lasers such as DBR structures[19,20] or polarization-maintaining fiber-based lasers[21]. Since the locking mechanism is based on the pump-power to signal frequency conversion, it could be interesting to compare 976 nm and 1470 nm pumping bands. Such dual-frequency stabilized lasers could provide all-fibered and integrated components for microwave photonics applications.

7. FUNDING

DGA (ANR-16-ASTR-0016); Région Bretagne, FEDER, Rennes Metropole (CPER SOPHIE-Photonique).

8. REFERENCES

[1] Fu, S., Shi, W., Feng, Y., Zhang, L., Yang, Z., Xu, S., Zhu, X., Norwood, R. A., Peyghambarian, N., “Review of recent progress on single-frequency fiber lasers,” J. Opt. Soc. Am. B 34(3), A49-A62 (2017).

[2] Loh, W. H., Laming, R. I., “1.55μm phase-shifted distributed feedback fibre laser,” Electron. Lett. 31(17), 1440-1442 (1995).

[3] Philipsen, J. L., Berendt, M. O., Varming, P., Lauridsen, V. C., Povlsen, J. H., Hubner, J., Kristensen, M., Palsdottir, B., “Polarisation control of DFB fibre laser using UV-induced birefringent phase-shift,” Electron. Lett. 34(7), 678–679 (1998).

[4] Ronnekleiv, E., Ibsen, M., Cowle, G. J., “Polarization characteristics of fiber DFB lasers related to sensing applications,” IEEE J. Quantum Electron. 36(6), 656–664 (2000).

[5] Hadeler, O., Ibsen, M., Zervas, M. N., “Distributed-feedback fiber laser sensor for simultaneous strain and temperature measurements operating in the radio-frequency domain,” Appl. Opt. 40(19), 3169–3175 (2001).

[6] Jin, L., Tan, Y.-N., Quan, Z., Li, M.-P., Guan, B.-O., “Strain-insensitive temperature sensing with a dual polarization fiber grating laser,” Opt. Express 20(6), 6021-6028 (2012).

[7] Leng, J. S., Lai, Y. C., Zhang, W., Williams, J. A. R., "A new method for microwave generation and data transmission using DFB laser based on fiber Bragg gratings," IEEE Photonics Technol. Lett. 18(16), 1729-1731 (2006).
[8] Maxin, J., Molin, S., Pillet, G., Morvan, L., Mugnier, A., Pureur, D., Dolfi, D., "Dual-frequency distributed feedback fibre laser for microwave signals generation," Electron. Lett. 47(14), 816–818 (2011).
[9] Yuan, Q., Liang, Y., Jin, L., Cheng, L., Guan, B.-O., "Implementation of a widely tunable microwave signal generator based on dual-polarization fiber grating laser," Appl. Opt. 54(4), 895-900 (2015).
[10] Liang, Y., Jin, L., Cheng, L., Guan, B.-O., "Stabilization of microwave signal generated by a dual-polarization DBR fiber laser via optical feedback," Opt. Express 22(24), 29356-29362 (2014).
[11] Keszenheimer, J. A., Zayhowski, J. J., Balboni, E. J., "Phase locking of 1.32-μm microchip lasers through the use of pump-diode modulation," Opt. Lett. 17(9), 649–651 (1992).
[12] Heurs, M., Quetschke, V. M., Willke, B., Danzmann, K., Freitag, I., "Simultaneously suppressing frequency and intensity noise in a Nd: YAG nonplanar ring oscillator by means of the current-lock technique," Opt. Lett. 29(18), 2148–2150 (2004).
[13] Brunel, M., Vallet, M., "Wavelength locking of CW and Q-switched Er 3+ microchip lasers to acetylene absorption lines using pump-power modulation," Opt. Express 15(4), 1612–1620 (2007).
[14] Guan, W., Marciante, J. R., "Pump-induced, dual-frequency switching in a short-cavity, ytterbium-doped fiber laser," Opt. Express 15(23), 14979–14992 (2007).
[15] Erdogan, T., Mizrahi, V., "Characterization of UV-induced birefringence in photosensitive Ge-doped silica optical fibers," JOSA B 11(10), 2100–2105 (1994).
[16] Kringlebotn, J. T., Archambault, J.-L., Reekie, L., Payne, D. N., "Er 3+: Yb 3+-codoped fiber distributed-feedback laser," Opt. Lett. 19(24), 2101–2103 (1994).
[17] Loh, W. H., Samson, B. N., Dong, L., Cowle, G. J., Hsu, K., "High performance single frequency fiber grating-based erbium: ytterbium-codoped fiber lasers," J. Light. Technol. 16(1), 114-118 (1998).
[18] Mo, S., Feng, Z., Xu, S., Zhang, W., Chen, D., Yang, T., Fan, W., Li, C., Yang, C., et al., "Microwave Signal Generation From a Dual-Wavelength Single-Frequency Highly Er^3+/Yb^3+ Co-Doped Phosphate Fiber Laser," IEEE Photonics J. 5(6), 5502306 (2013).
[19] Guan, B.-O., Zhang, Y., Zhang, L.-W., Tam, H.-Y., "Electrically Tunable Microwave Generation Using Compact Dual-Polarization Fiber Laser," IEEE Photonics Technol. Lett. 21(11), 727-729 (2009).
[20] Tan, Y.-N., Jin, L., Cheng, L., Quan, Z., Li, M., Guan, B.-O., "Multi-octave tunable RF signal generation based on a dual-polarization fiber grating laser," Opt. Express 20(7), 6961–6967 (2012).
[21] Liu, W., Jiang, M., Chen, D., He, S., "Dual-Wavelength Single-Longitudinal-Mode Polarization-Maintaining Fiber Laser and Its Application in Microwave Generation," J. Light. Technol. 27(20), 4455-4459 (2009).